Journal of Inorganic Biochemistry 105 (2011) 1580–1588

Contents lists available at SciVerse ScienceDirect

Journal of Inorganic Biochemistry

journal homepage: www.elsevier.com/locate/jinorgbio

Effects of terbium chelate structure on dipicolinate ligation and the detection of *Bacillus* spores

L.S. Barnes [a], K.R. Kaneshige [a], J.S. Strong [a], K. Tan [a], H.F. von Bremen [b], R. Mogul [a,*]

[a] Chemistry Department, California State Polytechnic University, Pomona, 3801 W. Temple Ave., Pomona, CA 91768, USA
[b] Department of Mathematics and Statistics, California State Polytechnic University, Pomona, 3801 W. Temple Ave., Pomona, CA 91768, USA

ARTICLE INFO

Article history:
Received 15 April 2011
Received in revised form 30 July 2011
Accepted 1 August 2011
Available online 14 September 2011

Keywords:
Terbium
Chelate
Dipicolinic
Bacillus
Anthrax
Luminescence

ABSTRACT

Terbium-sensitized luminescence and its applicability towards the detection of *Bacillus* spores such as anthrax are of significant interest to research in biodefense and medical diagnostics. Accordingly, we have measured the effects of terbium chelation upon the parameters associated with dipicolinate ligation and spore detection. Namely, the dissociation constants, intrinsic brightness, luminescent lifetimes, and biological stabilities for several Tb(chelate)(dipicolinate)$_x$ complexes were determined using linear, cyclic, and aromatic chelators of differing structure and coordination number. This included the chelator array of NTA, BisTris, EGTA, EDTA, BAPTA, DO2A, DTPA, DO3A, and DOTA (respectively, 2,2′,2″-nitrilotriacetic acid; 2,2-bis(hydroxymethyl)-2,2′,2″-nitrilotriethanol; ethylene glycol-bis(2-aminoethyl ether)-N,N,N′,N′-tetraacetic acid; ethylenediamine-N,N,N′,N′-tetraacetic acid; 1,2-bis(2-aminophenoxy)ethane-N,N,N′,N′-tetraacetic acid; 1,4,7,10-tetraazacyclododecane-1,7-diacetic acid; diethylenetriamine-N,N,N′,N″,N″-pentaacetic acid; 1,4,7,10-tetraazacyclododecane-1,4,7-triacetic acid; and 1,4,7,10-tetraazacyclododecane-1,4,7,10-tetraacetic acid). Our study has revealed that the thermodynamic and temporal emission stabilities of the Tb(chelate)(dipicolinate)$_x$ complexes are directly related to chelate rigidity and a ligand stoichiometry of $x = 1$, and that chelators possessing either aromaticity or low coordination numbers are destabilizing to the complexes when in extracts of an extremotolerant *Bacillus* spore. Together, our results demonstrate that both Tb(EDTA) and Tb(DO2A) are chemically and biochemically stable and thus applicable as respectively low and high-cost luminescent reporters for spore detection, and thereby of significance to institutions with developing biodefense programs.

1. Introduction

The use of terbium-sensitized luminescence for the detection of *Bacillus* spores, such as anthrax, has garnered much interest in recent years due its applications in biodefense [1,2] and microbial diagnostics [3,4]. The underlying strategy to the terbium-based detection is the formation of luminescent coordinate complexes between terbium (the reporter reagent) and dipicolinic acid, which is a secondary metabolite found in high abundance in *Bacillus* spores (5–15% by dry weight) [5]. In chemical terms, dipicolinic acid (DPA), pyridine-2,6-dicarboxylic acid, is a tridentate fluorophore that complexes terbium to form Tb(DPA)$_x$(H$_2$O)$_{9-3x}$, where $x = 1$, 2, and 3 [6,7]. These particular complexes are of spectroscopic significance as the triplet state of DPA transfers energy to bound terbium, ultimately resulting in long-lived luminescent emissions with large Stokes shifts in the visible spectrum [8,9]. For these reasons, therefore, DPA serves as an excellent biochemical marker and through use of sensitized lanthanide luminescence is fully applicable towards the development of rapid and cost-effective detection protocols for homeland security.

Essential to the reliable detection of DPA in the field or laboratory settings is the formation of chemically and biochemically stable terbium complexes of known stoichiometry, as biological extracts contain a multitude of metal-binding (and therefore metal-competitive) biomolecules and anions such as carbohydrates, peptides/proteins, gluconic acids, phosphate, oxalate, and more [10,11]. To date, however, $TbCl_3$ remains to be the most commonly used reagent for spore detection [1,12–14] despite its potential for rapid ligand exchange (or biochemical competition) due to the labile coordination sphere when dissolved in solution (Tb(H$_2$O)$_9$). As a consequence, the luminescence-based quantitative analysis of spore counts or DPA concentration are unnecessarily complicated, as complexes of mixed DPA stoichiometry, emission brightness, and emission lifetimes are formed under biological conditions.

To overcome these issues, therefore, the role of chelated terbium was recently introduced as an effective means in which to restrict the number of bound DPA and subsequently inhibit ligand competition [3,15]. While these reports clearly demonstrate the advantages of chelator-inclusion, there remains to be few, if any, studies in the literature that systematically address the effects of chelate structure and chelate

* Corresponding author.
E-mail address: rmogul@csupomona.edu (R. Mogul).

0162-0134/$ – see front matter © 2011 Elsevier Inc. All rights reserved.
doi:10.1016/j.jinorgbio.2011.08.020

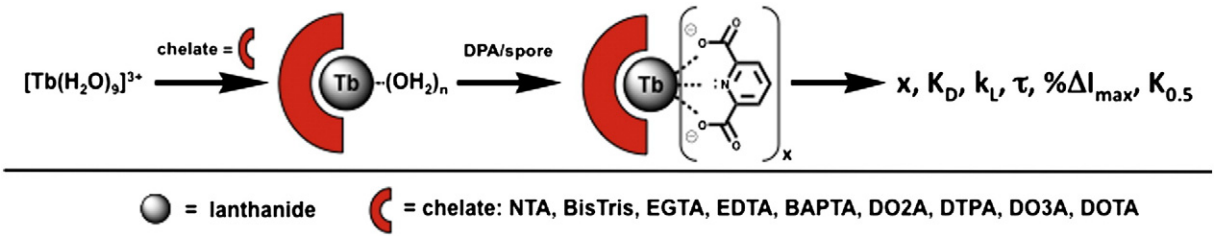

Scheme 1. Strategy designed to elucidate the effects of chelate structure upon the stoichiometry, formation, luminescence brightness, luminescence lifetime, and biological stability of terbium–dipicolinate complexes.

coordination number upon the formation and luminescence of terbium–dipicolinate complexes. Accordingly, we have studied an array of differing terbium chelates using the experimental strategy outlined in Scheme 1 and have elucidated the parameters of stoichiometry (x), formation (K_D), brightness (k_L), lifetime (τ), and biological stability ($\%\Delta I_{max}$, $K_{0.5}$) for several different Tb(chelate)$(DPA)_x$ complexes. Specifically, we have varied the chelate structure by utilizing the linear, cyclic, and aromatic chelators of NTA, BisTris, EDTA, EGTA, BAPTA, DO2A, DTPA, DO3A, and DOTA (Scheme 2), which together encompass the coordination number range of 4–8.

To our knowledge, this work represents the most holistic study to date regarding the effects of chelate structure and chelate coordination number upon terbium–dipicolinate complexes and the detection of extremotolerant *Bacillus* spores. Our analyses have revealed that chelate rigidity, coordination number, and ligand stoichiometry each independently impact the luminescence and biological stabilities of the differing Tb(chelate)$(DPA)_x$ complexes. Moreover, our biological luminescence stability studies were performed in extracts of the extremotolerant and sporulated form of *Bacillus pumilus* SAFR-032, which is a desiccation and radiation resistant microorganism originally isolated from the spacecraft assembly facilities at the Jet Propulsion Laboratory during construction of the Mars Phoenix lander [16–18]. Hence, our fundamental structural analysis of terbium chelation and its impact on spore detection has revealed both chemical and biochemical trends that have immediate application towards the development of reagents for NASA-related planetary protection endeavors, routine environmental monitoring, and first responder assays for homeland security.

2. Materials and methods

2.1. Materials

All chelates were purchased as the acid or free salt with the exception of DO2A and DO3A, which were obtained as the *t*-butyl protected esters: DPA (Alfa Aesar, 98%), NTA (EMD Chemicals, >98.0%), Bis–Tris (Acros Organics, 99+%), Na_4EDTA (Aesar, 98%), EGTA (Omnipur, >97%), BAPTA (Fluka Analytical, >95.0%), DO2A-*t*-Bu-ester (Macrocyclics), DTPA (Alfa Aesar 97%), DO3A-*t*-Bu-ester (Macrocyclics), and DOTA (Macrocyclics). Terbium (III) chloride hexahydrate (99.90%) and trifluoroacetic acid (99%) were purchased from Acros Organics. Sodium acetate trihydrate and 10× phosphate buffered saline (0.10 M total phosphate, 1.4 M NaCl, 27 mM KCl, pH 7.4) were purchased from VWR. All synthetic glassware were acid washed in a 1:1 mixture of HNO_3:H_2SO_4 for 1 hour at room temperature, thoroughly rinsed with ultrapure water and dried in an oven before use. All terbium stock solutions were prepared in 0.01 M HCl, whereas all ligation reactions were performed in filtered (0.22 μm) 0.10 M sodium acetate buffer (pH 5.5). Ultrapure water was used throughout (~18 MΩ/cm) for all aqueous solutions.

2.2. Synthesis of DO2A and DO3A

Deprotection of DO2A-*t*-Bu-ester (400.6 g/mol) and DO3A-*t*-Bu-ester (514.7 g/mol) (Macrocylics) were carried out in trifluoroacetic acid (TFA) as described. For each protected chelate, 80 mg were

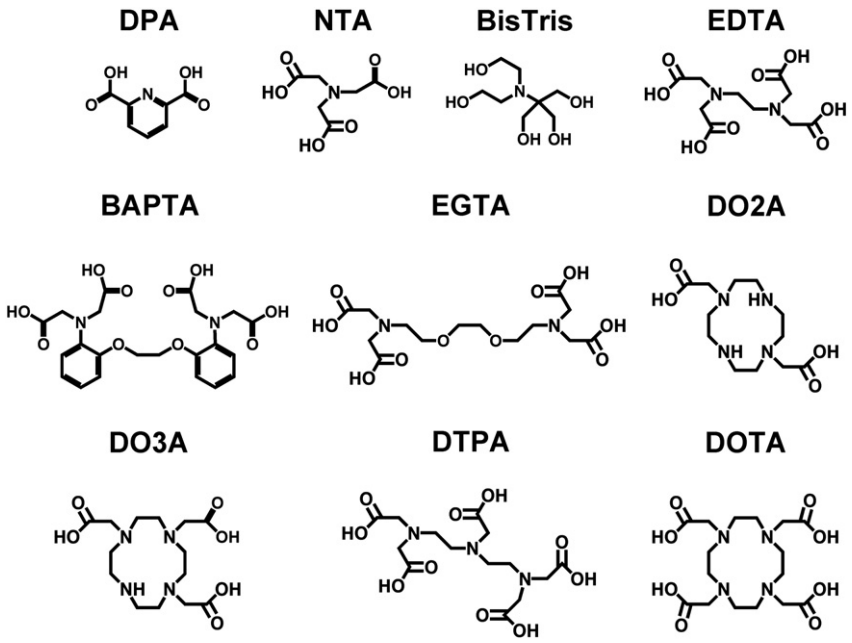

Scheme 2. Chelators and ligands listed in order of coordination number.

dissolved in 1.0 mL 95:5 TFA/H_2O in a 10 mL round-bottom flask and allowed to react at room temperature. After 2 hours, the sample was frozen under liquid N_2 and lyophilized for ~3 hours (VirTis Freeze Dryer 12XL). Upon completion, the sample was redissolved in 2.0 mL ultrapure water, re-frozen in liquid N_2, and re-lyophilized again for ~22 hours. The final product was retrieved with 95–97% yield with removal of the *t*-butyl group confirmed by absence of peaks in the ^{1}H NMR spectra at 1.418 and 1.421 ppm and in the ^{13}C NMR spectra at 38.716 and 28.243 ppm for DO2A and DO3A, respectively. Elemental analyses (%) provided molecular formulas of DO2A $(TFA)_{2.1}\cdot H_2O$ (C 35.56, H 5.33, F 21.94, N 10.08, O 27.09) and DO3A $(TFA)_{1.2}\cdot(H_2O)_2$ (C 38.78, H 6.10, F 11.63, N 11.55, O 31.94), which corresponded to molecular weights of 545.81 and 496.43 g/mol, respectively.

2.3. Formation of Tb(chelate) complexes

The varying complexes of Tb(chelate) in 1:1, 1:10, and 1:20 stoichiometric ratios were prepared using 1.0 mM $TbCl_3$ and 1.0 mM NTA, Bis–Tris, EDTA, EGTA, BAPTA, and DTPA; 10.0 mM EDTA, DO2A, and DOTA; and 20.0 mM DO3A. All metallations were performed in 0.10 M sodium acetate buffer (pH 5.5), thoroughly vortexed, and incubated at room temperature for 1 hour prior to use. All stock solutions were wrapped in aluminum foil and stored at −20 °C.

2.4. Emission and excitation luminescence

The emission (em) and excitation (ex) luminescence of the Tb(chelate) complexes in the presence of DPA were measured using a Jasco FP-6500 spectrofluorometer (medium sensitivity, 0.1 s response, 0.5 nm resolution, and 2000 nm/min). For all reactions, a stoichiometric ratio of 1:10 between Tb(chelate) (10 μM) and DPA (100 μM) was utilized in order to saturate the terbium ligation sphere. All reactions were 2.0 mL in volume, constantly stirred using a rotating magnetic bar, and performed in 0.10 M NaOAc (pH 5.5). Emission scans were obtained through excitation of DPA using a λ_{ex} (excitation) of 271 nm, an emission window of 450–700 nm, and slit widths of 3 nm (ex) and 1 nm (em). Excitation scans were obtained using a λ_{em} (emission) of 491 nm, an excitation window of 250–350 nm, and slit widths of 1 nm (ex) and 3 nm (em).

2.5. Luminescent titrations using dipicolinic acid

The ligation of DPA to each of the Tb(chelate) complexes was followed using luminescent titration experiments. These titrations were performed using 10 μM Tb(chelate) and a range of 0–150 μM DPA, which was added in 5 μM (from 0–60 μM) and 10 μM (from 60–150 μM) increments. The change in luminescence emission upon addition of the titrant was measured after 30 s of mixing; control experiments indicated no significant change in emission intensity with increased mixing times. All reactions were 2.0 mL in volume, conducted at room temperature, constantly stirred using a rotating magnetic bar, and performed in 0.10 M NaOAc (pH 5.5). The luminescence was measured on a Jasco FP-6500 (0.1 s response at low sensitivity) with a λ_{ex} of 271 nm, a λ_{em} of 491 nm, and slits width of 3 nm for both the excitation and emission windows. All luminescent data were corrected for inner filter effect to account for unbound DPA [19,20]. Subsequent modeling of the luminescent data by non-linear regression provided the parameters of dissociation constant (K_D) and intrinsic brightness (k_L) for each luminescent complex.

2.6. Luminescence and stability in Bacillus spore extracts

The ligation of DPA in *Bacillus* spore extracts was characterized using the terbium complexes of DO2A, EDTA, EGTA, BAPTA, NTA, and BisTris. Suspensions of sporulated *B. pumilus* SAFR-032 were obtained from P. Vaishampayan and K. J. Venkateswaran from the Jet Propulsion Laboratory (Pasadena, CA) [18]. Extracts were prepared by autoclaving 10 mL of a 1×10^7 cfu/mL spore suspension in sterile phosphate-buffered saline (10 mM total phosphate, 140 mM NaCl, 2.7 mM KCl, pH 7.4) for 30 min at 121 °C, followed by a 0.22 μm filtration step. The sensitized luminescence of the differing terbium chelates were then measured using 10 μM Tb(chelate) and a 20-fold dilution of the spore extract (an equivalent of 5×10^5 cfu/mL) in sterile filtered 0.10 M NaOAc buffer (pH 5.5). All reactions were 2.0 mL in volume, initiated by the addition of spore extract, and constantly stirred using a rotating magnetic bar. The sensitized luminescence resulting from the excitation of the spore-associated DPA (λ_{ex} of 271 nm) and concomitant emission from the terbium chelate (λ_{em} of 491 nm) was measured every 10 s over the span of 30 min using slits width of 3 nm for both the excitation and emission windows and a sensitivity of high on a Jasco FP-6500.

2.7. Luminescent lifetimes in control and Bacillus spore extracts

Luminescent lifetimes for the Tb(chelate) complexes were measured both in DPA and *Bacillus* control solutions. For the DPA control experiments, the Tb(chelate)$(DPA)_x$ complexes were prepared using stoichiometric ratios of 1:10 with 10 μM Tb(chelate) and 100 μM DPA. Lifetimes in D_2O were also measured for the NTA, BisTris, EDTA, and BAPTA analogs of Tb(chelate)$(DPA)_x$. The D_2O samples were prepared by removal of the aqueous solvent under vacuum using an Eppendorf SpeedVac (~5 hours on a setting of high) followed by dissolution of the dried salts in 0.75 mL D_2O (99.96%); the samples were then subjected to a second solvent removal step and the final dried lanthanide salts dissolved in an appropriate amount of D_2O. Luminescent lifetimes in the *Bacillus* spore extracts were also determined. These measurements were obtained by addition of 5×10^5 cfu/mL of the extract to 10 μM Tb(chelate) followed by 5 min of mixing. All lifetime reactions were 2.0 mL in volume, run at room temperature, and performed in 0.10 M NaOAc (pH 5.5). Lifetimes were measured on a Varian Cary Eclipse Fluorescence spectrofluorometer using a λ_{ex} of 271 nm, λ_{em} of 491 nm, delay time of 0.01 ms, gate time of 0.02 ms, decay time of 12 ms, and slits widths of 5 nm for both the excitation and emission windows.

3. Calculations

3.1. Regression analysis of the luminescent titrations

Mathematical modeling of the luminescent titration experiments were performed using Eq. (1), which relates emission intensity to the luminophore concentration *via* the intrinsic brightness term k_L. This term was derived from a simplification of Eq. (2) [20], where the terms of incident radiation power (P_0), quantum yield (Φ), molar absorptivity (ε), and path length (b) were combined to yield the overall term of k_L. Eq. (1) additionally incorporates the additive contribution of multiple luminescent species to the total intensity. A maximum of three species ($i=1$, 2, or 3) were used in our studies as terbium is typically nine-coordinate in water and dipicolinate is tricoordinate.

$$I = \sum_{i=1}^{3} k_{L_i}\left[\mathrm{Tb(complex)(DPA)}_i\right] \quad (1)$$

$$I = P_0\Phi(2.3\varepsilon bc) = (2.3P_0\Phi\varepsilon b)c = k_L c \quad (2)$$

Expressions for the concentrations of each luminophore (Tb(complex)$(DPA)_i$) were derived utilizing the mass balance relationships relating to mono-, bi-, and ter-chelation of DPA ($i=1$, 2, 3, respectively). For all regressions, the mass balance relationships possessed the general formulas displayed in Eqs. (3) and (4). It is important to

note that Tb(complex) refers to both the Tb(chelate) and $Tb(H_2O)_n$ complexes.

$$[DPA]_T = [DPA] + \sum_{i=1}^{3} [Tb(complex)(DPA)_i] \quad (3)$$

$$[Tb(complex)]_T = [Tb(complex)] + \sum_{i=1}^{3} [Tb(complex)(DPA)_i] \quad (4)$$

3.1.1. Mono-chelation of DPA

The formation of $Tb(chelate)(DPA)_1$ resulting from mono-chelation of DPA ($i=1$) was modeled using Eq. (5) for the hexadentate chelators of EDTA, EGTA, BAPTA, and DO2A.

$$I = k_L[Tb(chelate)(DPA)] \quad (5)$$

Accordingly, the mass balance relationships from Eqs. (3) and (4) for mono-chelation ($i=1$) were respectively expressed in terms of [DPA] and [Tb(chelate)] and substituted into the equilibrium dissociation expression (Eq. (6)).

$$K_D = \frac{[DPA][Tb(chelate)]}{[Tb(chelate)(DPA)]} \quad (6)$$

Upon substitution, this equilibrium expression was rearranged to yield Eq. (7) and subsequently solved using the quadratic formula as shown in Eq. (8). Substitution of the quadratic formula into Eq. (5) followed by use of the negative root provided very good fits to the luminescent data (KaleidaGraph®, Synergy Software).

$$[Tb(chelate)(DPA)]^2 - [Tb(chelate)(DPA)]K_D - [Tb(chelate)(DPA)][DPA]_T - [Tb(chelate)(DPA)][Tb(chelate)]_T + [DPA]_T[Tb(chelate)]_T = 0 \quad (7)$$

$$[Tb(chelate)(DPA)] = \frac{([DPA]_T + [Tb(chelate)]_T + K_D) \pm \sqrt{Q}}{2} \quad (8)$$

$$Q = ([DPA]_T + [Tb(chelate)]_T + K_D)^2 - 4[DPA]_T[Tb(chelate)]_T \quad (9)$$

3.1.2. Bis-chelation of DPA

The formation of $Tb(chelate)(DPA)_2$ resulting from bis-chelation of DPA ($i=2$) was modeled using Eq. (10) for the chelators of NTA and BisTris.

$$I = k_{L_1}[Tb(chelate)(DPA)] + k_{L_2}[Tb(chelate)(DPA)_2] \quad (10)$$

As described above, the mass balance relationships were substituted into the equilibrium association expressions for each DPA ligation to yield Eqs. (11) and (12). It should be noted that the association constants of K_{1-2} in the bis-ligation model were used as they provided a more streamlined algebraic derivation towards [Tb(chelate)$(DPA)_x$].

$$[Tb(chelate)(DPA)] = K_1[DPA][Tb(chelate)]_T/D \quad (11)$$

$$[Tb(chelate)(DPA)_2] = K_1K_2[DPA]^2[Tb(chelate)]_T/D \quad (12)$$

$$D = 1 + K_1[DPA] + K_1K_2[DPA]^2 \quad (13)$$

Subsequent substitution of these relationships into the DPA mass balance relationship in Eq. (3) ($i=2$) thus provided Eq. (14). In order to fit the data, this cubic equation was simultaneously substituted into Eq. (10) and numerically solved using a least-squares error method with internal constraints of $K_1 > K_2$ (MATLAB®, The MathWorks Inc.).

$$K_1K_2[DPA]^3 + (K_1 - K_1K_2[DPA]_T + 2K_1K_2[Tb(chelate)]_T)[DPA]^2 + (1 - K_1[DPA]_T + K_1[Tb(chelate)]_T)[DPA] - [DPA]_T = 0 \quad (14)$$

3.1.3. Ter-chelation of DPA

The formation of $Tb(DPA)_3$ resulting from the ter-chelation of DPA ($i=3$) was modeled using Eq. (15) for the aqua complex of $Tb(H_2O)_9$.

$$I = k_{L_1}[Tb(DPA)(H_2O)_6] + k_{L_2}[Tb(DPA)_2(H_2O)_3] + k_{L_3}[Tb(DPA)_3] \quad (15)$$

Utilizing the mass balance and equilibrium association expressions when $i=3$ the relationships displayed in Eqs. (16)–(18) were derived. Substitution of these expressions into the DPA mass balance relationship thus provided Eq. (20). Again, the association constants of K_{1-3} for the ter-ligation model were used as they provided a more streamlined algebraic derivation towards [Tb(chelate)$(DPA)_x$]. To fit the data, the quartic equation was simultaneously substituted into Eq. (15) and numerically solved using a least-squares error method. Regressions were performed using the internal constraints of $K_1 > K_2 > K_3$ and averages for all parameters derived from ten different spline interpolations using increments of 1–10 μM DPA (MATLAB®, The MathWorks Inc.).

$$[Tb(DPA)] = K_1[DPA][Tb]_T/D \quad (16)$$

$$[Tb(DPA)_2] = K_1K_2[DPA]^2[Tb]_T/D \quad (17)$$

$$[Tb(DPA)_3] = K_1K_2K_3[DPA]^3[Tb]_T/D \quad (18)$$

$$D = 1 + K_1[DPA] + K_1K_2[DPA]^2 + K_1K_2K_3[DPA]^3 \quad (19)$$

$$K_1K_2K_3[DPA]^4 + (K_1K_2 - K_1K_2K_3[DPA]_T + 3K_1K_2K_3[Tb]_T)[DPA]^3 + (K_1 - K_1K_2[DPA]_T + 2K_1K_2[Tb]_T)[DPA]^2 + (1 - K_1[DPA]_T + K_1[Tb]_T)[DPA] - [DPA]_T = 0 \quad (20)$$

3.2. Regression analysis of the luminescence biological stability

The biological stability of the differing Tb(DPA) complexes were modeled using a standard equation for a hyperbola (Eq. (21)), where $\%\Delta I_{max}$ related to the maximum change in intensity upon addition of the spores ($\%\Delta I_{max}$) and $K_{0.5}$ translated to the time required to reach half of this value. Note, that typical kinetic models did not sufficiently model the data and only hyperbolic fits to Tb(DO2A), Tb(EDTA), Tb(BAPTA), and Tb(NTA) were reproducibly obtained.

$$\%\Delta I_{change} = {}^{(\%\Delta I_{max}t)}\Big/_{(K_{0.5}+t)} \quad (21)$$

4. Results

4.1. Formation of Tb(chelate)$(DPA)_x$

In an effort to elucidate the impacts of chelate structure on Tb(chelate)$(DPA)_x$, we prepared several different complexes using the chelators of NTA, BisTris, EDTA, EGTA, BAPTA, DO2A, DO3A, DTPA, and DOTA (Scheme 2). Prior to any metallations, the cyclic chelators of DO2A, DO3A, and DOTA were prepared *via* deprotection of the *t*-

butyl protected esters in 95% aqueous TFA. The excitation and emission spectral profiles for each of the Tb(chelate)$(DPA)_x$ complexes are displayed in Fig. 1. The excitation scans displayed differing absorbances at the λ_{max} values of 271 and 279 nm, indicating both formation of the Tb(chelate) and subsequent DPA ligation for the complexes where chelate = NTA, BisTris, EDTA, EGTA, BAPTA, and DO2A. Emission scans for these complexes also confirmed energy transfer between the DPA donor and terbium acceptor through observance of luminescence emissions at 491 ($^7F_6 \leftarrow {}^5D_4$), 545 ($^7F_5 \leftarrow {}^5D_4$), 580 ($^7F_4 \leftarrow {}^5D_4$), and 625 nm ($^7F_3 \leftarrow {}^5D_4$). For Tb(DTPA), however, the similarities in excitation and emission profiles to that of $Tb(H_2O)_9$ were suggestive of weak chelation by DTPA and DPA. In contrast, the hepta- and octa-coordinate complexes of Tb(DO3A) and Tb(DOTA), which effectively excluded tridentate ligation of DPA, yielded no significant luminescence, thereby indicating that terbium–dipicolinate luminescence is necessarily dependent upon the formation of the coordinated complex.

4.2. Determination of K_D and k_L constants for Tb(chelate)$(DPA)_x$

The impacts of chelate structure on the formation and brightness of terbium–dipicolinate complexes are displayed in Fig. 2. In these experiments, the differing Tb(chelate) complexes as well as $Tb(H_2O)_9$ were titrated with DPA to form the differing complexes of Tb(chelate)$(DPA)_x(H_2O)_y$ and $Tb(DPA)_x(H_2O)_{9-3x}$, respectively. The luminescent titrations clearly demonstrate the impacts of chelate structure and coordination number as both the maximum intensities and shape of the titration curves change in comparison to the aqua control. Accordingly, three separate regression analyses were implemented in order to model the ligation of complexes possessing DPA stoichiometries of 1–3 DPA ligands ($x = 1$–3). As described further below, a mono-DPA model ($x = 1$) was utilized for titrations involving the hexadentate chelators, a bis-DPA model ($x = 2$) for the tetra- and penta-dentate chelators, and a ter-DPA model ($x = 3$) for unchelated or aqua terbium. The resulting regression parameters of DPA dissociation constant (K_D) and intrinsic brightness (k_L) for each luminescent Tb(chelate)$(DPA)_x$ complex are displayed in Table 1 and listed in order of chelate coordination number (CN).

As shown in Fig. 2A, the hexadentate chelators (CN = 6) of EDTA, EGTA, BAPTA, and DO2A were fitted used a mono-DPA chelation model, as the terbium center possessed only three open coordination sites (Tb(chelate)$(H_2O)_3$) that could be substituted by one tridentate DPA [15,21]. For these complexes, the trends in K_D revealed a direct relationship between complex stability and chelate rigidity (Tb(DO2A) $(15 \pm 1\ \mu M)$<Tb(BAPTA) $(33 \pm 4\ \mu M)$<Tb(EDTA) $(72 \pm 6\ \mu M)$<Tb(EGTA) $(110 \pm 5\ \mu M)$). Structural comparisons of the chelators suggested that rotational freedom is maximized in EGTA due to its ethylene glycol linker and sequentially restricted *via* the ethylene diamine group in EDTA, the sp^2 hybridized carbons in BAPTA, and the cyclic nature of DO2A [22,23]. Hence, our results demonstrated that the Tb(chelate)$(DPA)_1$ complex stability is directly related to the inclusion of rotationally-restricted chelators and perhaps the concomitant strong complexation of terbium. In contrast, chelate rigidity manifested an opposing effect on the intrinsic brightness (k_L) of the terbium–dipicolinate complexes, as indicated by the trends of Tb(EDTA) $(51 \pm 2) \approx$ Tb(EGTA) (50 ± 1)>Tb(BAPTA) (41 ± 2)>Tb(DO2A) (26 ± 1). Hence, the k_L results suggested that the structure of the terbium chelate structure impacted either the number of allowed transitions and/or quantum yield, as k_L is directly to both parameters *via* Eq. (2). Given that subtle

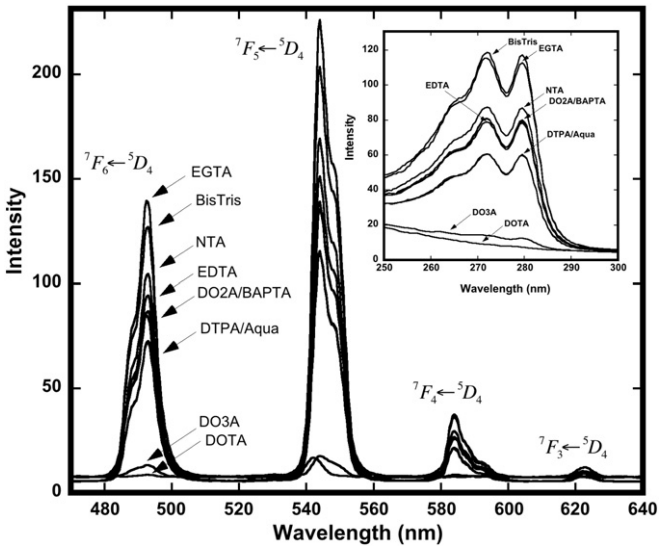

Fig. 1. Emission and excitation (inset) spectra of 10 μM Tb(chelate)$(DPA)_x$ in 0.10 M NaOAc (pH 5.5) using the conditions of $\lambda_{ex} = 271$ nm and a window of 450–700 nm for the emission spectra, and a $\lambda_{em} = 491$ nm and an excitation window of 250–350 nm for the inset spectra.

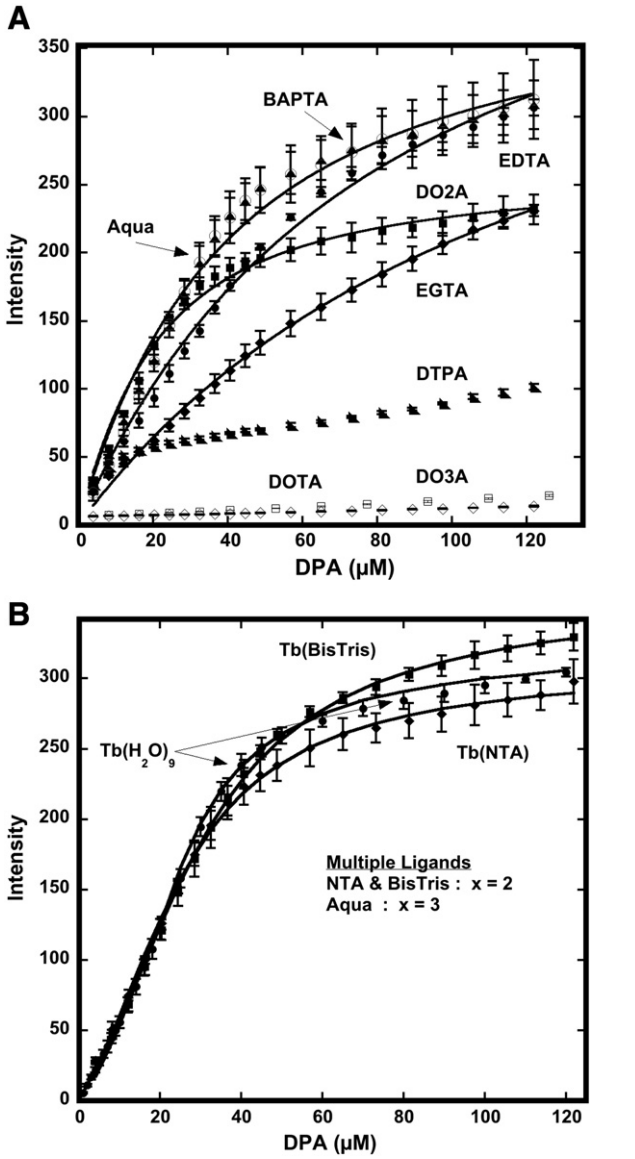

Fig. 2. Luminescence titrations of 10 μM Tb(complex) with 0–150 μM DPA ($\lambda_{ex} = 271$ nm, $\lambda_{em} = 491$ nm, 30 s mixing time), where complex included (A) the hexa, hepta, and octadentate chelators and regressions utilizing an $x = 1$ and (B) the tetra/pentadentate chelators and aqua control and regressions utilizing $x = 2$ and 3, respectively.

Table 1
Table of regression parameters for the Tb(chelate)$(DPA)_x$ complexes (standard deviations for $\tau(H_2O)$ and $\tau(D_2O)$ were ≤0.01 ms, for τ(spores) ≤0.09 ms, and $\%I_{max}$ ≤0.6%).

CN	Tb(chelate)	Tb(chelate)$(DPA)_n$	K_D (μM)	k_L	τH_2O (ms)	τD_2O (ms)	τspore (ms)	ΔI_{max}	$K_{0.5}$ (s)
0	$Tb(H_2O)_9$	$Tb(DPA)_1(H_2O)_6$	$>10^{-6}$	5.6 ± 0.4	–	–	–	−49%	100 ± 1
		$Tb(DPA)_2(H_2O)_3$	$\sim10^{-6}$	12 ± 1	–	–	–	–	–
		$Tb(DPA)_3$	11 ± 1	32 ± 1	2.02	–	0.88	–	–
4	Tb(NTA)	$Tb(NTA)(DPA)_1$	5.8 ± 1.8	6.2 ± 0.8	–	–	–	−40%	640 ± 16
		$Tb(NTA)(DPA)_2$	12 ± 2	31 ± 1	2.01	2.37	0.90	–	–
5	Tb(BisTris)	$Tb(BisTris)(DPA)_1$	14 ± 3	6.3 ± 3.3	–	–	–	−62%	80 ± 1
		$Tb(BisTris)(DPA)_2$	14 ± 3	38 ± 1	1.99	2.36	0.83	–	–
6	Tb(EDTA)	$Tb(EDTA)(DPA)_1$	72 ± 6	51 ± 2	2.01	2.37	0.85	−28%	570 ± 24
6	Tb(EGTA)	$Tb(EGTA)(DPA)_1$	110 ± 5	50 ± 1	1.99	–	–	−23%	140 ± 6
6	Tb(BAPTA)	$Tb(BAPTA)(DPA)_1$	33 ± 4	41 ± 2	2.01	2.40	1.08	−44%	630 ± 15
6	Tb(DO2A)	$Tb(DO2A)(DPA)_1$	15 ± 1	26 ± 1	2.01	–	2.01	+26%	14 ± 1
7	Tb(DO3A)	No significant ligation	n/a	n/a	n/a	n/a	n/a	n/a	n/a
8	Tb(DTPA)	$Tb(DTPA)(DPA)_1$	n/a	n/a	2.02	–	–	–	–
8	Tb(DOTA)	No significant ligation	n/a	n/a	n/a	n/a	–	n/a	n/a

structural variations in the aliphatic domains of terbium chelators have been found not to manifest significant changes in molar absorptivity [24], the change in k_L is therefore tentatively attributed to the variances in energy transfer between DPA and the terbium center possibly resulting from the differing degrees of ligation/chelation around the terbium center [25,26].

As shown in the Fig. 2B, the tetradentate and pentadentate chelators (CN = 4 and 5) of NTA [21,27] and BisTris [28] were fitted using the bis-DPA chelation model. As described below, our D_2O luminescent lifetime experiments on Tb(chelate)$(DPA)_x$ indicated no significant ligation of water when using a 10-fold excess of DPA over that of Tb(chelate). Regression using the bis-DPA chelation model was thereby warranted as a 12-fold excess of DPA over Tb was matched in all titration experiments. Hence, chelation of DPA to Tb(chelate)$(H_2O)_{4-5}$ yielded the sequential formation of Tb(chelate)(DPA)$(H_2O)_{1-2}$ followed by Tb(chelate)(DPA)(DPA′) when chelate = NTA or BisTris. In this scheme, however, coordination of the second DPA must occur through only mono or bi-dentate means as a result of the limited number of open sites on Tb(NTA)$(H_2O)_5$ and Tb(BisTris)$(H_2O)_4$. For simplicity's sake, however, the actual final product is herein abbreviated as Tb(chelate)$(DPA)_2$.

Thus, the trend in K_D for NTA and BisTris regarding the formation of Tb(chelate)$(DPA)_1$ was Tb(NTA) (5.8 ± 1.8 μM)<Tb(BisTris) (14 ± 3 μM), and for Tb(chelate)$(DPA)_2$ the trend was Tb(NTA) (12 ± 2 μM)≈Tb(BisTris) (14 ± 3 μM). In contrast, the intrinsic brightness terms (k_L) for Tb(chelate)$(DPA)_1$ were roughly equivalent for NTA and BisTris as Tb(NTA) (6.2 ± 0.8)≈Tb(BisTris) (6.3 ± 3.3). For Tb(chelate)$(DPA)_2$, however, the trend followed Tb(BisTris) (38 ± 1)>Tb(NTA) (31 ± 1). In summary, these results indicated that the inclusion of NTA, which is more structurally rigid than BisTris, manifested a clear increase in stability for Tb(chelate)$(DPA)_1$, similar to the effect observed for the hexadentate chelators. The trend in chelate rigidity also paralleled the opposing impact on brightness for Tb(chelate)$(DPA)_2$; however this result was perhaps additionally due to the weak and partial chelation of the second DPA.

Our analyses have additionally provided a preliminary regression of $Tb(H_2O)_9$ (the aqua control) and the related step-wise chelation by DPA to form $Tb(DPA)_1(H_2O)_6$, $Tb(DPA)_2(H_2O)_3$, and $Tb(DPA)_3$ (Fig. 2B). These analyses for $Tb(H_2O)_9$ are rather unique in that both the intrinsic brightness terms and formation constants for each luminescent complex ($Tb(DPA)_x(H_2O)_{9-3x}$, $x = 1–3$) were included in the computational and mathematical model. The least-squares type of regression, therefore, provided k_L values for $Tb(H_2O)_9$, $Tb(DPA)_2(H_2O)_3$, and $Tb(DPA)_3$ as well as a K_D value for $Tb(DPA)_3$ that were all low in error as calculated across three repeated trials and over several regression iterations. The K_D values for $Tb(DPA)_1(H_2O)_6$ and $Tb(DPA)_2(H_2O)_3$, however, are listed in Table 1 only as estimates as the calculated K_D values are significantly lower than the employed experimental concentration range and thus could not be accurately modeled. The values of $\sim10^{-6}$ μM for $Tb(DPA)_1(H_2O)_6$ and $\sim10^{-12}$ μM for $Tb(DPA)_2(H_2O)_3$ are therefore listed as upper limits, as larger values concomitantly provided increased errors in all parameters. Current efforts are focused upon redevelopment of our model in order to better address this issue.

Nevertheless, the regressions allowed for direct comparison of the stepwise formation of $Tb(DPA)_3$ or the full chelation of 1, 2, and 3 DPA ligands to terbium. The results demonstrated that the K_D for fully chelated DPA in $Tb(DPA)_3$ decreased by ~6-orders of magnitude for each successive DPA dissociation. This dramatic decrease in K_D is clearly related to the number of open coordination sites on terbium, which increased by three with each respective DPA dissociation. Additionally, these results revealed that full chelation of DPA imparted significant stability to the terbium complex, as the approximate K_D for the 2nd and partially chelated DPA in both Tb(NTA)$(DPA)_2$ and Tb(BisTris)$(DPA)_2$ was $\sim10^{1}$ μM, whereas for $Tb(DPA)_2(H_2O)_3$ the K_D for the 2nd and fully chelated DPA was $\sim10^{-6}$ μM. Furthermore, the results demonstrated that luminescence brightness was not directly related to the number of bound DPA sensitizers as the intrinsic brightness for $Tb(DPA)_3$ was lower than that of Tb(chelate)$(DPA)_1$, when chelate = EDTA, BAPTA, EGTA, and DO2A.

Lastly, the hepta and octa-coordinate chelates of Tb(DO3A), Tb(DTPA), and Tb(DOTA) (CN = 7 and 8), despite not being modeled, provided additional insights into the impact of chelate structure (Fig. 2A). For example, both Tb(DO3A) and Tb(DOTA) provided no appreciable luminescent intensities due to exclusion of DPA from the coordination spheres; which thus offered further evidence that terbium–dipicolinate luminescence is necessarily dependent upon formation of the coordinated complex. For Tb(DTPA), however, the DPA ligation was reproducibly measured but not reliably modeled due to weak chelation by DTPA, as suggested in control excitation and emission studies. This is significant as both DTPA and DOTA are octa-coordinate, yet only the rigid and rotationally-restricted platform of DOTA provided the stable chelation of terbium.

4.3. Luminescence and stability in Bacillus spore extracts

In order to reveal the impacts of chelate structure on *Bacillus* detection, the change in luminescence intensities for several different terbium chelates were measured in the presence of sporulated *B. pumilus* SAFR-032. In these experiments, extracts of *B. pumilus* SAFR-032 were mixed with Tb(chelate) (where chelate = DO2A, EDTA, EGTA, BAPTA, BisTris, NTA, or water) and the change in luminescence measured every 10 s over the course of 30 min. As displayed in Fig. 3, the initial intensities of each Tb(chelate) increased rather significantly upon addition of the spores (30 s after addition), thus confirming that sensitization of terbium occurred through excitation of the spore-associated biochemical

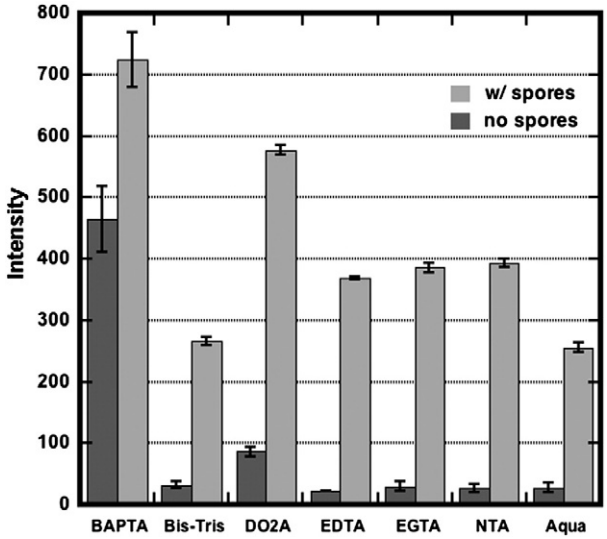

Fig. 3. Initial change in terbium luminescence after addition of extracts of *B. pumilus* SAFR-032 spores to the Tb complexes ($\lambda_{ex} = 271$ nm, $\lambda_{em} = 491$ nm, 30 s after addition of spores).

constituents, namely DPA. The emission intensities in the spore extracts followed the trend of DO2A>NTA≥EGTA≥EDTA>BAPTA> Aqua≥BisTris, which did not correlate with the trends in k_L, thus indicating the presence of metal competition arising from the biological extract. Moreover, the luminescent intensities for each Tb(chelate) complex differentially changed over time, which revealed that the biological stability of the luminescence (and related DPA binding) were directly linked to chelation of the terbium ion. As shown in Fig. 4, all complexes except for Tb(DO2A) manifested minor to major losses in intensity over time, which revealed that competition arising from non-sensitizing and metal-binding biomolecules were significant for *Bacillus* extracts of this type. In sharp contrast, the intensities for Tb (DO2A) rose over time [2] confirming that ligation/chelation of DPA to the macrocyclic terbium chelate was kinetically slow but subsequently stable to biological competition. Lastly, standard first and second-order kinetic models did not sufficiently model the data, which provided additional support for multiple competitions arising from the biological extract.

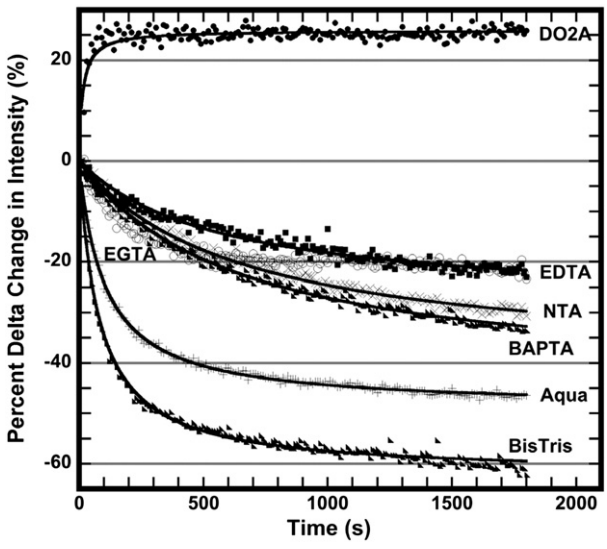

Fig. 4. Temporal change in terbium luminescence during incubation in extracts of *B. pumilus* SAFR-032 ($\lambda_{ex} = 271$ nm , $\lambda_{em} = 491$ nm, 10 s intervals).

Mathematical description of the biological stability plots were therefore afforded using a hyperbolic model that provided the maximum percent change in intensity ($\%\Delta I_{max}$) resulting from the competition and the time required to reach half of this maximum value ($K_{0.5}$). Complexes possessing lower $\%\Delta I_{max}$ (*e.g.* lowest losses in intensity) and larger $K_{0.5}$ values (*e.g.* increased stability over time) were generally considered to be biologically stable and suitable for *Bacillus* detection. Thus, our regressions provided $\%\Delta I_{max}$ and $K_{0.5}$ values of Tb(DO2A) (+26%, ~14 s), Tb(EGTA) (−23%, ~140 s), Tb (EDTA) (−28%, ~570 s), Tb(NTA) (−40%, ~640 s), Tb(BAPTA) (−44%, ~630 s), $Tb(H_2O)_9$ (−49%, ~100 s), and Tb(BisTris) (−62%, ~80 s). In summary, these parameters revealed that the overall intensities for Tb(EGTA), $Tb(H_2O)_9$, and Tb(BisTris) decreased by a factor of 0.5 in less than ~2 min after mixing ($K_{0.5} \leq 140$ s), which rendered these complexes as inadequate for stable *Bacillus* detection. In contrast, the complexes of Tb(EDTA), Tb(NTA), and Tb(BAPTA) were much more stable with $K_{0.5}$ values of 540–640 s (~10 min), whereas for Tb(DO2A) the intensities increased over time ($\%\Delta I_{max} = +26\%$) and reached the maxima within 1 min. However, for the Tb complexes that accommodated binding of 2–3 DPA ligands (Tb(NTA), Tb (BisTris), and $Tb(H_2O)_9$) or contained aromatic functional groups (Tb(BAPTA)), the trends in $\%\Delta I_{max}$ revealed large overall intensity losses, which additionally rendered these complexes as unsuitable for *Bacillus* detection. The analysis, therefore, revealed that the most stable and best suited Tb complexes to be Tb(DO2A), due to its positive $\%\Delta I_{max}$ value, and Tb(EDTA), due its relatively low loss in intensity and general stability over time ($\%\Delta I_{max} = -28\%$, $K_{0.5} = \sim 570$ s).

4.4. Luminescent lifetimes in spore extracts

The impact of chelate structure on the luminescence lifetimes of several Tb (chelate)$(DPA)_x$ complexes were determined in H_2O, D_2O, and in spore extracts using temporal methods. As displayed in Table 1, the aqueous lifetimes for all Tb(DPA) complexes were ~2.0 ms, which suggested that all coordination sites were occupied by either the ligand or chelator. Further support of this hypothesis was gained from D_2O experiments, which provided no significant evidence for water ligation under our experimental conditions [21,24]. Hence, this supported a DPA stoichiometry of $x = 2$ for the complexes of Tb(NTA)$(DPA)_x$ and Tb(BisTris)$(DPA)_x$, though in each case we propose only partial chelation of the second DPA ligand.

The biological impact on the lifetime was also assessed *via* incubation of the terbium complexes in the *Bacillus* extracts for 5 min. The lifetimes of all complexes except Tb(DO2A) decreased to the range of ~0.85–1.08 ms, due to the formation of luminescent side products between sensitizing biomolecules and the terbium complexes. The Tb(DO2A) complex, however, manifested no change in lifetime when incubated in spore samples, which thus provided additional evidence towards the extreme stability of the Tb(DO2A)(DPA) complex.

5. Discussion

The application of Tb complexes as reporter reagents for the detection of anthrax (*Bacillus anthracis*) is necessarily dependent upon rapid and reliable detection of dipicolinate. As biological assays typically require several hours to days for completion, the development of rapid first responder protocols for the assessment of biothreat are of paramount importance. However, as all *Bacillus* spores contain dipicolinate and due to the sensitizing properties of various bio-related chemicals [29–31], these terbium reagents are best suited for the purpose of initial assessment, or to confirm the need for subsequent and more in-depth microbiological and genetic assays. The aim of this work, therefore, has been to identify the structure/function relationships between the Tb(chelate) reporter and the parameters of spore detection that allow for the development of cost-effective protocols for first responders that require detection times of ≤10 min.

As a control microorganism, we have focused exclusively on *B. pumilus* SAFR-032, which was isolated in the spacecraft assembly facilities at the Jet Propulsion Laboratory and found to possess extreme tolerances towards oxidative stress and gamma and ultraviolet radiation. This microorganism, therefore, served as a non-pathogenic and environmentally-relevant control as its extremotolerances are attributed to the efficient metabolism of exogenous reagents [16]. Hence, we have systematically elucidated the effects of terbium chelation upon the parameters required for stable spore detection, namely, the formation, brightness, lifetimes, and biological stabilities of several Tb(chelate)$(DPA)_x$ complexes in both control solutions and in extracts of *B. pumilus* SAFR-032.

The array of chelators utilized in this study has ultimately revealed the fundamental impacts of linear, cyclic, and aromatic chelate structures as well as chelate coordination number, which ranged from 4 to 8. As demonstrated, the biochemical competition in extracts of *B. pumilus* SAFR-032 was very chelate-dependent with the relatively more rotationally-restricted hexadentate chelators of EDTA and DO2A providing the best thermodynamic and emission stabilities over time. In contrast, both the complex stabilities and brightness were minimized when utilizing the low coordination number chelators of NTA and BisTris, the rotationally-flexible hexadentate chelator of EGTA, and the aromatic hexadentate chelator of BAPTA. Stable complexation with DPA was also not observed for the higher coordination number chelators of DO3A and DOTA due to exclusion of DPA the coordination sphere, thus confirming the requisite need for terbium coordination by DPA for this luminescence method. Moreover, biological stability was significantly impacted by DPA stoichiometry with mono-chelation of DPA ($x=1$) providing the complexes most resistant towards biochemical competition. Thus, our combined analyses highlight the structural determinants of non-aromaticity, rotational-restriction, and hexadentate coordination along with mono-analyte binding as the major factors underlying the functional strength and stability of detecting dipicolinate in *Bacillus* spore extracts.

Our chelate analyses in control DPA solutions additionally revealed that terbium–dipicolinate stability is directly dependent upon both chelate rigidity and the number of open coordination sites. For example, the lowest dissociation constants were obtained from complexes containing the highest number of open coordination sites (Tb(hexadentate chelate)$(H_2O)_3$>Tb(BisTris)$(H_2O)_4$>Tb(NTA)$(H_2O)_5$>Tb(DPA)$(H_2O)_6$>Tb$(H_2O)_9$), whereas for the hexadentate series, the decrease in dissociation constant was directly related to chelate rigidity (Tb(EGTA)>Tb(EDTA)>Tb(BAPTA)>Tb(DO2A)). However, the trend in thermodynamic stabilities ($1/K_D$) was not reflected under biological conditions, where the presence of aromatic groups and multiple bound waters yielded complexes that were unstable and susceptible to ligand competition. As expected, the intrinsic brightness of the complexes not only were generally inversely related to the number of bound waters but also were surprisingly inversely related to chelate rigidity, which may provide some insight into the energy transfer mechanisms of terbium sensitization. Lastly, we report that terbium luminescence is not directly proportional to the number of coordinated sensitizers, as the brightest observed luminophores in our work were the ternary metal complexes that possessed DPA stoichiometries of $x=1$ and a requisite hexadentate chelator.

6. Conclusions

We propose that Tb(EDTA) or Tb(DO2A) are both suitable complexes for use as potential first responder reagents. Our demonstration of increased chemical and biological stabilities through chelation is rather significant as most studies to date employ $TbCl_3$ as the reporter reagent, which under our conditions is extremely susceptible to *Bacillus* biochemical competition. Our comparative approach and determination of the K_D, τ_{spore}, $\%\Delta I_{max}$, and $K_{0.5}$ values clearly indicate that Tb(DO2A) provides the most sensitive and stable complexation of DPA under biological conditions, due to the noted impact of chelate rigidity and potential for hydrogen bonding with DPA [15] in solution. For nations or institutions with limited budgets, however, the costs associated with DO2A synthesis (*e.g.* purchase and deprotection of the DO2A-*t*-butyl ester, purification *via* lyophilization, and analysis by NMR) may prohibit the wide-spread dissemination of Tb(DO2A) as a first responder reagent. Our work, therefore, highlights the use of Tb(EDTA) as a reasonable chemical alternative due to its relatively low K_D value, millisecond luminescent lifetime, and moderate stability in biological extracts. Moreover, the commercial availability of EDTA, ease of Tb(EDTA) preparation, and our simplified spectral techniques (*e.g.* no requirement for filters or high-resolution fluorometers) together add to the feasibility of fabricating low-cost assays for those nations or institutions with developing biodefense programs.

Abbreviations

DPA	dipicolinic acid or pyridine-2,6-dicarboxylic acid
NTA	2,2′,2″-nitrilotriacetic acid
BisTris	2,2-bis(hydroxymethyl)-2,2′,2″-nitrilotriethanol
EDTA	ethylenediaminetetraacetic acid
BAPTA	1,2-bis(2-aminophenoxy)ethane-N,N,N′,N′-tetraacetic acid
EGTA	ethylene glycol-bis(2-aminoethyl ether)-N,N,N′,N′-tetraacetic acid
DO2A	1,4,7,10-tetraazacyclododecane-1,7-diacetic acid
DO3A	1,4,7,10-tetraazacyclododecane-1,4,7-triacetic acid
DTPA	diethylenetriamine-N,N,N′,N″,N″-pentaacetic acid
DOTA	1,4,7,10-tetraazacyclododecane-1,4,7,10-tetraacetic acid

Acknowledgements

We thank the following institutions for their support: the California State University Program for Education and Research in Biotechnology (CSUPERB) Faculty–Student Collaborative Research Seed Grant Program, NASA Astrobiology Institute-Minority Institution Research Program (NAI-MIRS), and Cal Poly Pomona's new investigator funds. We also extend our gratitude to Parag Vaishampayan and Kasthuri Venkateswaran from the Jet Propulsion Laboratory for preparation of the *B. pumilus* SAFR-032 extracts.

References

[1] A.A. Hindle, E.A.H. Hall, Analyst 124 (1999) 1599–1604.
[2] M.L. Cable, J.P. Kirby, D.J. Levine, M.J. Manary, H.B. Gray, A. Ponce, Journal of the American Chemical Society 131 (2009) 9562–9570.
[3] A. Gültekin, A. Ersöz, N. Sarıözlü, A. Denizli, R. Say, Journal of Nanoparticle Research 12 (2010) 2069–2079.
[4] R. Kort, A.C. O'Brien, I.H. van Stokkum, S.J. Oomes, W. Crielaard, K.J. Hellingwerf, S. Brul, Applied and Environmental Microbiology 71 (2005) 3556–3564.
[5] J.C. Lewis, Analytical Biochemistry 19 (1967) 327–337.
[6] G. Jones, V.I. Vullev, J. Phys, Chemical A 106 (2002) 8213–8222.
[7] D.L. Rosen, S. Niles, Applied Spectroscopy 55 (2001) 208–216.
[8] C. Turro, K.L.F. Patty, P.M. Bradley, in: A. Sigel, H. Sigel (Eds.), Metal Ions in Biological Systems, Lanthanide Ions as Luminescent Probes of Proteins and Nucleic Acids, vol. 40, Marcel Dekker, Inc, New York, 2003.
[9] G. Jones, V.I. Vullev, Photochemistry and Photobiology Science 1 (2002) 925–933.
[10] S. Mounicou, J. Szpunar, R. Lobinski, Chemical Society Reviews 38 (2009) 1119–1138.
[11] I. Bertini, Biological Inorganic Chemistry: Structure and Reactivity, University Science Books, Sausalito, 2007.
[12] W.W. Yang, A. Ponce, International Journal of Food Microbiology 133 (2009) 213–216.
[13] D.L. Rosen, Applied Optics 45 (2006) 3152–3157.
[14] P.M. Pellegrino, N.F. Fell Jr., D.L. Rosen, J.B. Gillespie, Analytical Chemistry 70 (1998) 1755–1760.
[15] M.L. Cable, J.P. Kirby, K. Sorasaenee, H.B. Gray, A. Ponce, Journal of the American Chemical Society 129 (2007) 1474–1475.
[16] J. Gioia, S. Yerrapragada, X. Qin, H. Jiang, O.C. Igboeli, D. Muzny, S. Dugan-Rocha, Y. Ding, A. Hawes, W. Liu, L. Perez, C. Kovar, H. Dinh, S. Lee, L. Nazareth, P. Blyth, M. Holder, C. Buhay, M.R. Tirumalai, Y. Liu, I. Dasgupta, L. Bokhetache, M. Fujita, F. Karouia, P. Eswara Moorthy, J. Siefert, A. Uzman, P. Buzumbo, A. Verma, H. Zwiya, B.D. McWilliams, A. Olowu, K.D. Clinkenbeard, D. Newcombe, L. Golebiewski, J.F. Petrosino, W.L. Nicholson, G.E. Fox, K. Venkateswaran, S.K. Highlander, G.M. Weinstock, PloS One 2 (2007) e928.

[17] D.A. Newcombe, A.C. Schuerger, J.N. Benardini, D. Dickinson, R. Tanner, K. Venkateswaran, Applied and Environmental Microbiology 71 (2005) 8147–8156.
[18] L. Link, J. Sawyer, K. Venkateswaran, W. Nicholson, Microbial Ecology 47 (2004) 159–163.
[19] M.M. Puchalski, M.J. Morra, R. von Wandruszka, Fresenius' Journal of Analytical Chemistry 340 (1991) 341–344.
[20] J.R. Lakowicz, Principles of Fluorescence Spectroscopy, Springer, New York, 2010.
[21] W.D. Horrocks, D.R. Sudnick, Journal of the American Chemical Society 101 (1979) 334–340.
[22] A. Yuchi, M. Hirai, H. Wada, G. Nakagawa, Chemistry Letters 19 (1990) 773–776.
[23] M. Meyer, V. Dahaoui-Gindrey, C. Lecomte, R. Guilard, Coordination Chemistry Reviews 178–180 (1998) 1313–1405.
[24] M. Li, P.R. Selvin, Journal of the American Chemical Society 117 (1995) 8132–8138.
[25] L. Oyang, H.-L. Sun, X.-Y. Wang, J.-R. Li, D.-B. Nie, W.-F. Fu, S. Gao, K.-B. Yu, Journal of Molecular Structure 740 (2005) 175–180.
[26] J.-G. Kang, M.-K. Na, S.-K. Yoon, Y. Sohn, Y.-D. Kim, I.-H. Suh, Inorganica Chimica Acta 310 (2000) 56–64.
[27] J.G. Kang, J.P. Hong, S.K. Yoon, J.H. Bae, Y.D. Kim, Journal of Alloys and Compounds 339 (2002) 248–254.
[28] K.N. Nicholson, S.A. Wood, Journal of Solution Chemistry 31 (2002) 703–717.
[29] T.L. Esplin, M.L. Cable, H.B. Gray, A. Ponce, Inorganic Chemistry 49 (2010) 4643–4647.
[30] J. Georges, Analyst 118 (1993) 1481–1486.
[31] T. Steinkamp, U. Karst, Analytical and Bioanalytical Chemistry 380 (2004) 24–30.